Biochimica et Biophysica Acta 1778 (2008) 2091–2096

Contents lists available at ScienceDirect

Biochimica et Biophysica Acta

journal homepage: www.elsevier.com/locate/bbamem

The effects of lipids on the structure of the eukaryotic cytolysin equinatoxin II: A synchrotron radiation circular dichroism spectroscopic study

Andrew J. Miles [a,1], Alison Drechsler [b,c,1], Katarina Kristan [d,2], Gregor Anderluh [d], Raymond S. Norton [c], B.A. Wallace [a], Frances Separovic [b,*]

[a] Department of Crystallography, Birkbeck College, University of London, London WC1E 7HX, UK
[b] School of Chemistry, Bio21 Institute, University of Melbourne, VIC 3010, Australia
[c] The Walter and Eliza Hall Institute of Medical Research, 1G Royal Parade, Parkville VIC 3050, Australia
[d] Department of Biology, Biotechnical Faculty, University of Ljubljana, Večna pot 111, 1000 Ljubljana, Slovenia

ARTICLE INFO

Article history:
Received 21 February 2008
Received in revised form 27 March 2008
Accepted 1 April 2008
Available online 8 April 2008

Keywords:
Cytolysin
Synchrotron radiation circular dichroism (SRCD) spectroscopy
Secondary structure
Protein–lipid interactions
Equinatoxin II
Phospholipid membrane

ABSTRACT

Synchrotron radiation circular dichroism (SRCD) spectroscopy studies of the eukaryotic pore-forming protein equinatoxin II (EqtII) were carried out in solution and in the presence of micelles or small unilamellar vesicles (SUV) of different lipid composition. The SRCD structural data was correlated with calcein leakage from SUV and with partitioning of EqtII to liposomes, and micelles, according to haemolysis assays. The structure of EqtII in water and dodecylphosphocholine micelles as determined by SRCD was similar to the values calculated from crystal and solution structures of the protein, and no changes were observed with the addition of sphingomyelin (SM). SM is required to trigger pore formation in biological and model membranes, but our results suggest that SM alone is not sufficient to trigger dissociation of the N-terminal helix and further structural rearrangements required to produce a pore. Significant changes in conformation of EqtII were detected with unsaturated phospholipid (DOPC) vesicles when SM was added, but not with saturated phospholipids (DMPC), which suggests that not only is membrane curvature important, but also the fluidity of the bilayer. The SRCD data indicated that the EqtII structure in the presence of DOPC:SM SUV represents the 'bound' state and the 'free' state is represented by spectra for DOPC or DOPC:Chol vesicles, which correlates with the high lytic activity for SUV of DOPC:SM. The SRCD results provide insight into the lipid requirements for structural rearrangements associated with EqtII toxicity and lysis.

1. Introduction

Equinatoxin II (EqtII) is a member of the actinoporin family of sea anemone toxins that function by forming pores in cell membranes by a multi-step mechanism, which includes membrane binding, conformational change and oligomerisation [1]. The resulting oligomeric pores, which consist of most likely four monomers, have a radius of about 1 nm [2,3].

The structure of EqtII consists of two short helices packed against opposite faces of a β-sandwich structure formed by two five-stranded β-sheets [4,5]. The current model of pore formation proposes that EqtII binds to the membrane initially via the aromatic-rich region [6–8], then the N-terminal α-helical region is transferred to the lipid membrane [6,9,10] and, finally, across the bilayer to form a functional pore [8,9,11]. The structural details of the final oligomeric assembly are not known, but it is clear that pore formation by the actinoporins is quite distinct from the mechanisms adopted by various classes of bacterial pore-forming toxins [12].

The actinoporins are highly basic proteins of approximately 20 kDa. In model membranes their level of lytic activity depends on the lipid composition of the target membrane, with lytic activity being enhanced dramatically by the presence of sphingomyelin (SM) [2,3]. However, it has also been suggested that presence of cholesterol [13] or lipid domains in the absence of SM [14] may increase permeabilising activity. It is thus not yet clear if SM may act as a specific receptor for the toxin in the lipid membranes or whether the membrane physical properties enable EqtII to form pores. Some recent studies provided data that support the former possibility: the interaction of EqtII with model lipid membranes composed of dimyristoylphosphatidylcholine (DMPC) and SM has been investigated by solid-state NMR [15], which indicated a preferential interaction between the toxin and SM. Furthermore, solution NMR studies of the interaction of EqtII containing fluorinated tryptophans with lipid micelles and bicelles identified perturbations in particular regions of the protein in the presence of SM [16]. However, a key result was that the ^{19}F resonance of W149 did not change, even in the presence of SM. Thus, interaction with SM in these model membranes was not sufficient to trigger dissociation of the N-terminal helix from the β-sandwich,

* Corresponding author. Tel.: +61 3 8344 2447; fax: +61 3 9347 5180.
E-mail address: fs@unimelb.edu.au (F. Separovic).
[1] These authors contributed equally.
[2] Present Address: Medical Faculty, University of Maribor, Slomškov trg 15, 2000 Maribor, Slovenia.

0005-2736/$ – see front matter © 2008 Elsevier B.V. All rights reserved.
doi:10.1016/j.bbamem.2008.04.001

which would expose W149, suggesting that the mere presence of SM was not sufficient to produce the changes associated with pore formation in the absence of a bilayer.

Fourier transform infrared (FTIR) and circular dichroism (CD) spectroscopy studies of actinoporins have examined structural changes of actinoporins upon membrane association. Both methods detected small increases in β-sheet and α-helical content at the expense of random structure in the presence of unilamellar phospholipid vesicles [17–21]. However, in the FTIR studies, SM contributes to the amide signal in the same region as proteins and hence it is difficult to interpret the data unambiguously as being due to changes in the protein structure. In addition, CD spectroscopy in vesicle systems can be difficult to interpret because of differential light scattering effects present due to the lipid vesicles [22]. Moreover, the lipid:protein ratios required to eliminate absorption flattening artifacts [23] and to reproduce conditions that support pore formation *in vitro* result in low protein concentrations. These produce spectra with low signal/noise ratios that make detection and interpretation of small changes difficult. However, synchrotron radiation circular dichroism (SRCD) spectroscopy is able to overcome these problems by utilising a detector geometry that reduces apparent light scattering [24]. In addition, its higher sensitivity enables the use of smaller amounts of protein and the high light throughput means that the lipids, which generally do not produce a significant CD signal but do have significant absorbance in the far UV region of the spectrum, do not degrade the quality of the spectra. Furthermore the ability to acquire data down to lower wavelengths (around 175 nm instead of 190 nm) provides more accurate secondary structure information [25], due to the additional spectroscopic differences between secondary structural types at the low wavelengths, as is evident in representative SRCD spectra of 'standard' protein structures [24].

In this study the secondary structures of EqtII in aqueous solution, micelles, and small unilamellar vesicles (SUVs) of different lipid compositions were determined using SRCD in order to gain a better understanding of the structural changes in the toxin in the presence of model membranes. SM, which is required for lytic activity of EqTII, was added to both phosphocholine micelles and DMPC vesicles and the effect on EqtII structure was examined. To determine the effect of lipid order on the toxin, cholesterol was included and SUV of an unsaturated phospholipid were studied.

2. Materials and methods

2.1. Materials

Dodecylphosphocholine (DPC), dioleoylphosphatidylcholine (DOPC), dimyristoyl phosphatidylcholine (DMPC) and brain sphingomyelin (SM) were from Avanti Polar Lipids (Alabaster, AL), and cholesterol (Chol) was from Sigma (St Louis, MI).

EqtII was expressed in *Escherichia coli* and purified essentially as described previously [26].

2.2. Sample preparation

For DPC micelles, DPC was dissolved in deionised (MilliQ) water at a concentration of 2.4 mg/ml (5.7 mM). For SUV samples and the DPC:SM (5:1, mol:mol) sample, lipids were dissolved in 25% methanol/75% chloroform (v/v) then combined at the desired ratios. Solvents were removed by rotary evaporation to produce a lipid film, which was dried under vacuum. Lipid films were suspended in deionised water and vortexed with glass beads to produce multilamellar vesicles (MLV) at a concentration of ~5 mg/ml. Prior to data collection, ~800 μL aliquots of the MLV dispersions were removed by pipette and sonicated on ice for 30 min with a 20 s on/off cycle, to produce a clear suspension of SUVs. Lipid samples were mixed with 46 μL of EqtII stock solution (10 mg/ml) and the pH values of all solutions were adjusted to between 6.5 and 7.0. The samples were centrifuged at ~6000 ×g for 2 min to remove any large vesicles and then de-gassed for 15 min to remove any oxygen that would absorb in the vacuum ultraviolet (VUV) region of the spectra.

Sample concentrations were 0.46 mg/mL for EqtII and 3.8–4.8 mg/mL for the different SUV lipid mixtures, in all cases corresponding to an approximate molar ratio of 1:250 EqtII:lipid. This proportion was chosen for comparison to our earlier solid-state NMR studies and electron microscopy of MLV carried out at this protein/lipid ratio, which showed significant bilayer disruption [15]. The EqtII concentration was calculated from the A_{280}, using a molar extinction coefficient of 36,100 $M^{-1}cm^{-1}$ [27].

2.3. Synchrotron radiation circular dichroism (SRCD) spectroscopy

SRCD spectra were acquired on beamline CD12 (SRS, Daresbury Laboratory, UK), in a 0.02 cm pathlength Suprasil quartz cell (Hellma UK Ltd, Southend on Sea, UK). Typically, spectra were measured at 25 °C, over the wavelength range 280–175 nm, using an interval of 1 nm and a dwell time of 1 s, with three repeat scans of each sample. The SRCD spectra are presented here in mean residue ellipticity units (degrees cm^2 $decimol^{-1}$) against wavelength (nm). Spectra were processed using CDTool [28]; for each type of sample and baseline (containing the appropriate lipid), triplicate measurements were averaged, the averaged baseline was subtracted from the averaged sample spectra and the final plot was smoothed with a Savitsky-Golay filter. The instrument was calibrated at the beginning of each synchrotron beam injection using camphorsulfonic acid (CSA), as described previously [29]. SUV stability was verified by comparison of the baseline SRCD and high tension (HT) spectra (the latter being a type of pseudoabsorption spectrum) obtained both before and after sample acquisition, with changes in these spectra suggesting vesicle instability or aggregation.

2.4. Analysis of SRCD data

The secondary structure content was calculated using the DICHROWEB server [30] with the CDSSTR [31], CONTINLL [32] and SELCON3 [33] algorithms. The normalized root mean square deviation (NRMSD) [34] was calculated as a goodness-of-fit parameter. The SP175 reference dataset [35] was used for the structure calculations reported as it includes more representative types of structures and also generally produced lower NRMSD values than did other available reference data sets [33]. An average of the results from the three algorithms is reported with +/− values being the standard deviations in the secondary structures calculated by the three methods. The error bars on the plots represent the standard deviations in the repeated measurements.

2.5. Permeabilisation of small unilamellar vesicles

Small unilamellar vesicles (SUVs) were prepared as described previously [9] by sonicating a solution of multilamellar liposomes prepared in the presence of 80 mM

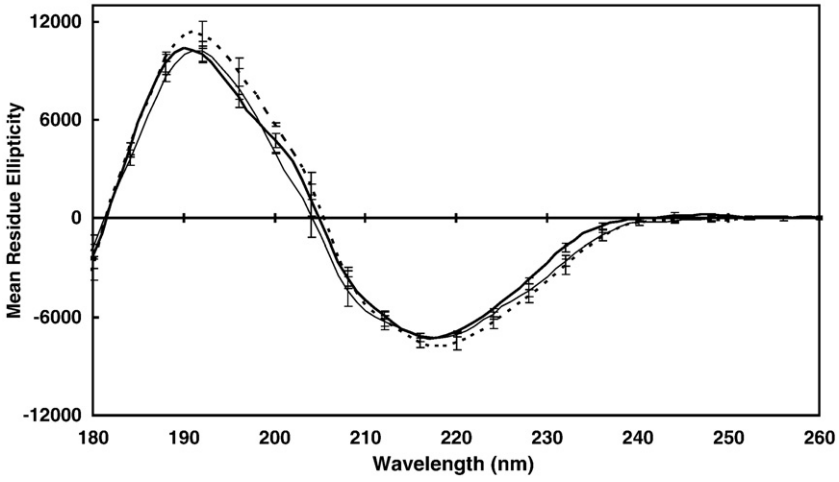

Fig. 1. SRCD spectra of EqtII in H_2O (thick solid line), DPC (thin solid line) and DPC:SM (5:1) (dashed line), at a 1:250 EqtII:lipid ratio. [EqtII] 0.46 mg/ml, pH 7.0, 25 °C, 0.02 cm cell.

Table 1
Calculated secondary structure of EqtII based on SRCD data and estimation of amount of bound toxin in water, micelles and SUV

EqtII system	helix	sheet	Bound EqtII[a]
Water	9% (±4)	44% (±4)	–
DPC micelles	11% (±4)	39% (±4)	0%
DPC:SM (5:1) micelles	9% (±4)	43% (±3)	100%
DOPC SUV	9% (±4)	39% (±3)	0%
DOPC:Chol (2:1) SUV	6% (±3)	43% (±2)	0%
DOPC:SM (1:1) SUV	9% (±3)	47% (±2)	91% (±5)
DOPC:SM:Chol (8:1:1) SUV	7% (±3)	47% (±2)	70% (±12)
DMPC SUV	10% (±3)	42% (±3)	0%
DMPC:SM (1:1) SUV	10% (±3)	42% (±2)	49% (±6)
DMPC:SM:Chol (1:1:1) SUV	6% (±2)	44% (±2)	97% (±1)

[a] Bound EqtII based on haemolysis assay, $n=3\pm$S.D.

calcein (20 mM Hepes, pH 7, adjusted by NaOH). Multilamellar liposomes were sonicated for 30 min with 10 s on and off cycles. After that, vesicles were centrifuged at top speed in a benchtop centrifuge at room temperature and incubated at 45 °C for 30 min. Lipid compositions used were DOPC, DOPC:SM (1:1), DOPC:Chol (2:1), DOPC:SM:Chol (8:1:1), DMPC, DMPC:SM (1:1) and DMPC:SM:Chol (1:1:1, mol:mol). To remove untrapped calcein, the vesicles were applied to a small Superdex G-50 column, equilibrated in 20 mM Tris–HCl, 1 mM EDTA, pH 7.

Vesicle permeabilisation by EqtII was assayed in a 1.5 mL cuvette (Jasco FP-750 Fluorimeter, Tokyo, Japan). Lipid vesicles at 58 μM final concentration were stirred at 25 °C in 20 mM Tris–HCl, 1 mM EDTA, pH 7, then toxin was added at 250:1 mole ratio (0.23 μM) and fluorescence was followed for 20 min. The maximal release was obtained by the addition of 2 mM Triton X-100 at the end of the assay. No lysis was observed from SUV without addition of EqtII. The excitation and emission wavelengths were 485 and 520 nm, respectively; both slits were set to 5 nm. The percentage of calcein release (R%) was calculated as follows:

$$R\% = (F_{fin}-F_{in})/(F_{max}-F_{in}) \times 100$$

where F_{in} and F_{fin} represent the initial and final (steady-state) values of fluorescence before and after peptide addition. F_{max} is the fluorescence after the addition of 2 mM Triton X-100.

2.6. Determination of the bound toxin

The amount of lipid-associated EqtII was estimated by titrating the remaining free toxin in a microtiter plate hemolytic assay. EqtII at 0.23 μM concentration and various lipid preparations at 58 μM (lipid/toxin molar ratio around 250) were incubated for 10 min at room temperature in final 200 μL volume of 130 mM NaCl, 20 mM Tris–HCl, pH 7.4. Then the mixture was diluted two-fold across the microtiter plate and 100 μL of bovine red blood cell suspension (A_{630}=0.5) was added. The haemolysis was followed at 630 nm for 20 min. The remaining haemolytic activity was compared to the control EqtII solution, which did not contain any lipids. Mixed lipid micelles and SUV without EqtII did not induce haemolysis. Three replicates were done for each lipid preparation.

3. Results

3.1. EqtII in water and micelles

SRCD spectra of EqtII dissolved in water and in DPC and DPC:SM (5:1) micelles are shown in Fig. 1. In water, the calculated secondary structure of the protein was 9% (±4%) helix and 44% (±4%) sheet, which compares well with the structure determination by NMR (7% helix and 36% sheet) [5] and X-ray crystallography (12% helix and 46% sheet) [4]. There was no significant difference in the experimental plots for EqtII in water and in DPC or DPC:SM micelles, which all fall within the error bars (Table 1) and have the same shape curves (Fig. 1). However, based on the haemolysis assay (Section 2.6 above), no toxin appeared to bind to pure DPC (resulting in 100% haemolysis by unbound toxin) while 100% bound to DPC:SM micelles (resulting in no haemolysis).

The calculated values for the secondary structure of EqtII in micelles also did not show significant differences from that in water, implying that micelles are not sufficient to induce a change in structure, and that the physical environment of a bilayer may be required. Note that calculations were also carried out with a new reference dataset that included membrane proteins [36], but the results were essentially identical to those using the SP175 reference dataset.

3.2. EqtII with DOPC, SM and Chol bilayers

The SRCD spectra of EqtII added to SUV of DOPC, DOPC:Chol (2:1), DOPC:SM (1:1), and DOPC:SM:Chol (8:1:1) are shown in Fig. 2. The addition of EqtII to DOPC:SM:Chol (1:1:1) resulted in the visible disruption of the vesicles with formation of a white precipitate; therefore, this composition was not analyzed. Lipid bilayers composed of equimolar unsaturated PC, SM and Chol are thought to contain microdomains or 'rafts' [37], and the addition of EqtII may have led to vesicle instability and aggregation.

The SRCD spectra with DOPC together with SM or Chol were significantly different from each other as revealed by the shapes of the curves (with notable increases in magnitude and shifts of the low wavelength (~190 nm) peak to higher wavelengths when SM was present). The spectrum of EqtII in DOPC was approximately the same as that for DOPC:Chol. However, the DOPC:SM spectrum was radically different, with the DOPC:SM:Chol being intermediate between the two. Indeed, principal component analyses [35] showed that the latter was an average of the other two spectra, which were represented by two distinct principal components. This suggests that the DOPC:SM and the DOPC alone (and to a good approximation DOPC:Chol)

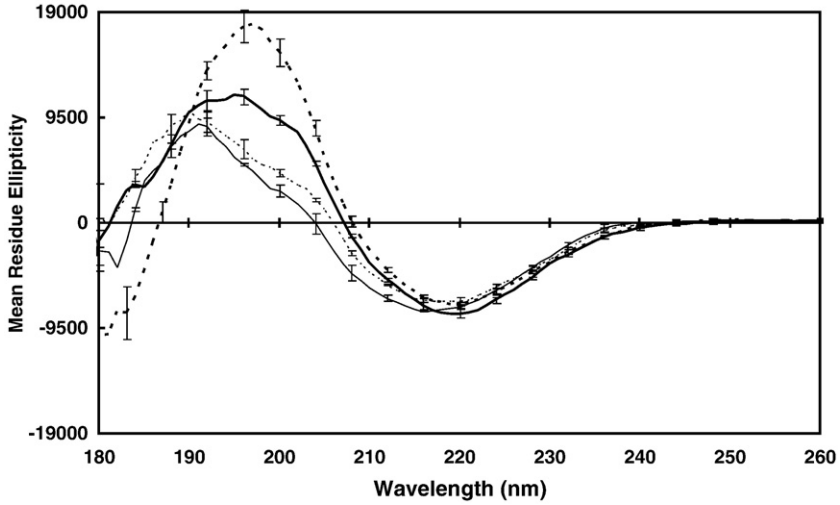

Fig. 2. SRCD spectra of EqtII in DOPC (thin solid line), DOPC:SM (1:1) (dashed line) DOPC:Chol (2:1) (dotted line) and DOPC:SM:Chol (8:1:1) (thick solid line) at a 1:250 EqtII:lipid ratio. [EqtII] 0.46 mg/ml, pH 7.0, 25 °C, 0.02 cm cell.

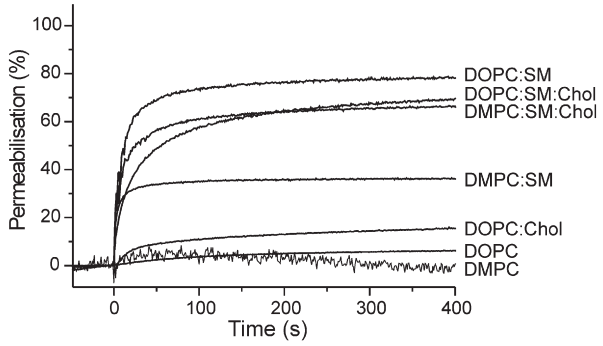

Fig. 3. Lysis of SUV by EqtII. The figure shows the kinetics of calcein release upon addition of the toxin to a final 0.23 μM concentration (at a lipid/toxin ratio ~250) at time 0 s. The permeabilisation is expressed as a percentage of release as compared to the one obtained by the addition of 2 mM Triton X-100 at the end of the assay. The representative trace of two measurements is shown.

represent two forms, which may be the "bound" and "free" states, and that the DOPC:SM:Chol sample is an equilibrium mixture of the two states. EqtII binding to DOPC vesicles, based on haemolysis testing (Table 1), appeared to occur only when SM was present, with 0% binding for DOPC and DOPC:Chol (2:1), 91±5% bound for DOPC:SM (1:1), and 70±12% bound for DOPC:SM:Chol (8:1:1).

The calculated secondary structures for the DOPC alone sample were 9±4% for helix and 39±3% sheet, whereas the SUVs with SM showed a significant increase in β-sheet content with values for both DOPC:SM (1:1) and DOPC:SM:Chol (8:1:1) being 47±2% sheet. (Table 1). All lipid compositions used for SRCD were also tested for calcein release at the same lipid/toxin molar ratio (Fig. 3). DOPC vesicles with Chol showed a small increase in leakage when EqtII was added and maximal lysis was seen for DOPC:SM (1:1) vesicles, followed by DOPC:SM:Chol (8:1:1), consistent with this interpretation.

3.3. EqtII with DMPC, SM and Chol bilayers

For comparison, a more ordered phospholipid, the saturated DMPC, was used instead of the unsaturated DOPC. The spectra for DMPC:Chol (2:1) and DMPC:SM:Chol (8:1:1) acquired before and after data acquisition of the EqtII-lipid samples changed due to vesicle instability and, therefore, the SRCD spectra were not used. The SRCD spectra of EqtII with DMPC, DMPC:SM (1:1) and DMPC:SM:Chol (1:1:1) SUV are shown in Fig. 4. The spectrum with DMPC alone is very similar to that with DOPC alone and would appear to be of the "free" state. The SRCD spectrum for DMPC:SM:Chol (1:1) showed a small difference in shape, which correlates with the lack of overlap of the error bars on the plots, especially in the low wavelength (~190 nm) peak. This difference is much less than even the "intermediate" DOPC:SM:Chol spectrum and suggests an equilibrium with only a small component (<10%) of the "bound" state. In addition, there were only small changes in the calculated secondary structure that were not significant with respect to the standard deviations in the calculations, i.e. helix changed from 10±3% to 6±2% and sheet changed from 42±3% to 44±2% (Table 1). EqtII did not appear to bind to DMPC, but ~50% (49±6%) bound to DMPC:SM (1:1) and almost 100% (97±1%) to DMPC:SM:Chol (1:1:1) vesicles based on the haemolysis assay (Table 1). The binding results correlate well with the calcein release data (Fig. 3), where SUV of DMPC showed no leakage when EqtII was added, while DMPC:SM and DMPC:SM:Chol showed medium and high calcein release, respectively.

4. Discussion

The SRCD analyses indicated that the secondary structure of EqtII in water is ~9% helical and 44% sheet, which is intermediate between the NMR solution structure (7% helix and 36% sheet) and the X-ray crystal structure (12% helix and 46% sheet). The solution structure [5] was calculated without TALOS-based backbone dihedral angle restraints, which are now used routinely and which provide more extensive and more accurate definition of backbone conformation than the combination of NOEs and coupling-constant-based angle restraints used for EqtII. Hence, the backbone angles in the solution structure deviate more from the values used to define canonical secondary structure. However, if the crystal [4] and solution structures are superimposed, they agree very well in the regions of the β-strands. The well-defined region of the N-terminal helix coincides almost exactly in the solution and crystal structures (i.e. residues 15–26). Moreover, the crystal structure is a dimer, and the two EqtII molecules are in contact through their N-terminal regions, so there is the potential for some distortion of local structure. In the solution structure, the second helix spanned residues 129–134 and is longer in the crystal structure (130–138). The most significant difference between the NMR and X-ray derived structures occurs around residues 134–138, where the solution structure is not well-defined and the crystal structure may be affected by intermolecular contacts in this region. Nevertheless, the SRCD analyses yield secondary structure contents that are consistent with the solution and crystal values, and validate the use of the method for examining the secondary structure of this protein.

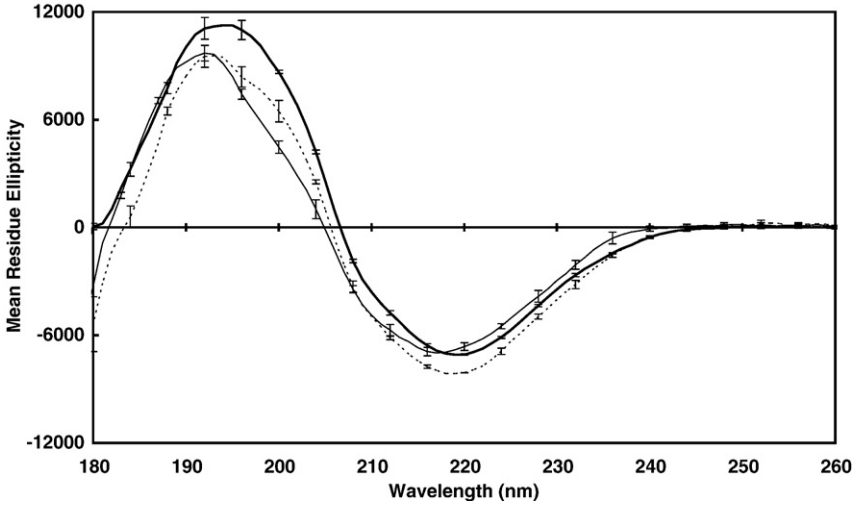

Fig. 4. SRCD spectra of EqtII in DMPC (thin solid line), DMPC:SM (1:1) (dotted line) and DMPC:SM:Chol (1:1:1) (thick solid line) at a 1:250 EqtII:lipid ratio. [EqtII] 0.46 mg/ml, pH 7.0, 25 °C, 0.02 cm cell.

The SRCD studies also indicated that in the presence of DPC micelles, either with or without SM present, no significant net secondary structural change occurs. ^{19}F NMR data [16] suggested that with DPC:SM micelles the N-terminal region of EqtII did not dissociate from the bulk of the protein. Local changes were detected in the region of Trp112 when SM was added to DPC, but this localized type of change would not be detected by SRCD. Both studies, however, suggest that the mere presence of SM is not in itself sufficient to cause a major conformational change, which may require the presence of a lipid bilayer structure.

The results for SUV with unsaturated and saturated PC contrasted with those in micelles, where the conformation of the toxin appeared to be the same as for EqtII in aqueous solution. The interactions of EqtII with SUV composed of the unsaturated phospholipid DOPC, DOPC:SM (1:1), DOPC:Chol (2:1) and DOPC:SM:Chol (8:1:1) were studied. Vesicles with equimolar Chol and SM were used since Chol favours phase-separation of SM [38] and formation of lipid raft-like domains [37]. For comparison, interaction with the saturated phospholipid DMPC, DPMC:SM (1:1) and DPMC:SM:Chol (1:1:1), which formed stable SUV, was also studied. The DOPC vesicles with SM and Chol form a disordered liquid crystalline phase whereas DMPC vesicles with SM and Chol would be in a more ordered phase [39], which may prevent the toxin inserting and resulting in a similar secondary structure content as for EqtII in water. The main gel–fluid phase transition temperature for DOPC is low (−17 °C) compared to DMPC (23 °C) [40], so that SUV of DMPC:Chol (2:1) and DMPC:SM:Chol (8:1:1) were unstable at 25 °C [41,42] and, therefore, data from these DMPC samples were not used. SUV of DOPC with SM and Chol were more stable, but when EqtII was added to DOPC:SM:Chol (1:1:1) SUV, a precipitate formed, suggesting that the toxin led to aggregation of the vesicles.

When EqtII was added to DMPC:SM:Chol (1:1:1) vesicles, binding appeared to increase to almost 100% and a significant spectral change was detected. This change, which involved only the low wavelength region (and, therefore, would not have been detectable with conventional CD spectroscopy), does not appear to correlate with the expected increase in helix content and concomitant decrease in β-sheet (see below). Paradoxically, the shift to higher wavelengths in the 190 nm region (Fig. 4) would be consistent with an increase in β-sheet, although this would not be consistent with the increase in magnitude. However, the shift may in fact be attributable to several other features: 1) association with membranes can cause spectral red-shifting of the ~190 nm peak [43], so the observed difference could be partially attributable to this, although the magnitude of the shift observed is larger than expected; 2) interaction of structural elements can produce low wavelength (<200 nm) changes detectable by SRCD but not readily detectable by conventional CD [44]; and 3) significant changes in aromatic environments can have some effect in the low wavelength region of the spectrum normally attributed only to secondary structure. This may result from local changes in the vicinity of the fluorinated Trp residues of EqtII observed in the presence of lipid micelles by ^{19}F NMR [16].

When the toxin interacts with lipid bilayers, the largest change in structure is likely to be the result of dissociation of the N-terminal region from the β-sandwich and concomitant association with the lipid in a helical conformation [9,11,45]. This conformational change is necessary for pore formation, but is probably not sufficient, as the functional pore requires the association of most likely four EqtII molecules to form a tetramer. From the present SRCD data we are unable to distinguish between the conformational changes associated with lipid binding and those associated with pore formation (the latter correlating with lytic activity), but we can detect a significant conformational change that occurs in the DOPC bilayers when SM is present. This is consistent with the observation that EqtII does not lyse DOPC or DOPC:Chol significantly but does lyse DOPC:SM and DOPC:SM:Chol vesicles (Fig. 3). EqtII added to DOPC:SM and DOPC:SM:Chol showed the greatest change in conformation by SRCD (Fig. 2). The observed differences in structure and binding observed may be related to the order of the lipid, with DOPC being the more fluid and possibly allowing protein unfolding or insertion into the bilayer in the presence of Chol and SM.

Although no toxin appeared to be bound to pure DPC micelles, 100% was bound and no longer active in haemolysis assays when EqtII was added to DPC:SM (5:1) micelles. These results are thus in agreement with the current model of EqtII interaction with membranes, where the toxin interacts with DPC only via the exposed residues, including Trp112, from the broad loops at the bottom of the molecule, but dissociation of the N-terminal helix to the lipid membrane and further structural rearrangements to produce a pore structure does not occur. The SRCD data indicate that the EqtII structure represents the 'bound' state in the case of DOPC:SM and the 'free' state for DMPC vesicles, which correlates with high and no lytic activity, respectively. The changes in conformation of EqtII detected in the more unsaturated phospholipid, DOPC, suggest that not only is membrane curvature important, but also the fluidity of the bilayer. Taken together, these studies suggest that SM alone is not sufficient to trigger dissociation of the N-terminal helix, which may require the context of a fluid bilayer.

In summary, SRCD studies of EqtII in solution, micelles and lipid bilayers of different composition have provided insight into the lipid requirements for structural changes associated with toxicity and lysis. Such studies could not have been done using conventional CD spectroscopy, as they required high lipid/protein ratios, the presence of lipid bilayers, and the ability to measure data accurately at low wavelengths.

Acknowledgements

Supported by grants from the BBSRC to BAW, Slovenian Research Agency to GA, Australian Research Council to FS, and by a beamtime grant from the CCLRC to FS and a CCLRC joint programme mode access grant to BAW and R.W. Janes (Queen Mary, Univ. of London). RSN is supported by a fellowship from the Australian National Health and Medical Research Council.

References

[1] G. Anderluh, P. Maček, Cytolytic peptide and protein toxins from sea anemones (Anthozoa: Actiniaria), Toxicon 40 (2002) 111–124.
[2] G. Belmonte, C. Pederzolli, P. Maček, G. Menestrina, Pore formation by the sea anemone cytolysin equinatoxin II in red blood cells and model lipid membranes, J. Membr. Biol. 131 (1993) 11–22.
[3] M. Tejuca, M. Dalla Serra, M. Ferreras, M.E. Lanio, G. Menestrina, Mechanism of membrane permeabilization by sticholysin I, a cytolysin isolated from the venom of the sea anemone *Stichodactyla helianthus*, Biochemistry 35 (1996) 14947–14957.
[4] A. Athanasiadis, G. Anderluh, P. Maček, D. Turk, Crystal structure of the soluble form of equinatoxin II, a pore-forming toxin from the sea anemone *Actinia equina*, Structure 9 (2001) 341–346.
[5] M.G. Hinds, W. Zhang, G. Anderluh, P.E. Hansen, R.S. Norton, Solution structure of the eukaryotic pore-forming cytolysin equinatoxin II: implications for pore formation, J. Mol. Biol. 315 (2002) 1219–1229.
[6] G. Anderluh, A. Barlič, Z. Podlesek, P. Maček, J. Pungerčar, F. Gubenšek, M.L. Zecchini, M. Dalla Serra, G. Menestrina, Cysteine-scanning mutagenesis of an eukaryotic pore-forming toxin from sea anemone: topology in lipid membranes, Eur. J. Biochem. 263 (1999) 128–136.
[7] P. Malovrh, A. Barlič, Z. Podlesek, P. Maček, G. Menestrina, G. Anderluh, Structure–function studies of tryptophan mutants of equinatoxin II, a sea anemone pore-forming protein, Biochem. J. 346 (2000) 223–232.
[8] Q. Hong, I. Gutiérrez-Aguirre, A. Barlič, P. Malovrh, K. Kristan, Z. Podlesek, P. Maček, D. Turk, J.M. González-Mañas, J.H. Lakey, G. Anderluh, Two-step membrane binding by equinatoxin II, a pore-forming toxin from the sea anemone, involves an exposed aromatic cluster and a flexible helix, J. Biol. Chem. 277 (2002) 41916–41924.
[9] P. Malovrh, G. Viero, M. Dalla Serra, Z. Podlesek, J.H. Lakey, P. Maček, G. Menestrina, G. Anderluh, A novel mechanism of pore formation: membrane penetration by the N-terminal amphipathic region of equinatoxin, J. Biol. Chem. 278 (2003) 22678–22685.
[10] I. Gutierrez-Aguirre, A. Barlic, Z. Podlesek, P. Maček, G. Anderluh, J.M. Gonzalez-Manas, Membrane insertion of the N-terminal alpha-helix of equinatoxin II, a sea anemone cytolytic toxin, Biochem. J. 384 (2004) 421–428.
[11] K. Kristan, Z. Podlesek, V. Hojnik, I. Gutiérrez-Aguirre, G. Gunčar, D. Turk, J.M. González-Mañas, J.H. Lakey, P. Maček, G. Anderluh, Pore formation by equinatoxin,

a eukaryotic pore-forming toxin requires a flexible N-terminal region and a stable β-sandwich, J. Biol. Chem. 279 (2004) 46509–46517.
[12] M.W. Parker, S.C. Feil, Pore-forming protein toxins: from structure to function, Prog. Biophys. Mol. Biol. 88 (2005) 91–142.
[13] V. de los Rios, J.M. Mancheno, M.E. Lanio, M. Onaderra, J.G. Gavilanes, Mechanism of the leakage induced on lipid model membranes by the hemolytic protein sticholysin II from the sea anemone *Stichodactyla helianthus*, Eur. J. Biochem. 252 (1998) 284–289.
[14] A. Barlic, I. Gutierrez-Aguirre, J.M. Caaveiro, A. Cruz, M.B. Ruiz-Arguello, J. Perez-Gil, J.M. Gonzalez-Manas, Lipid phase coexistence favors membrane insertion of equinatoxin-II, a pore-forming toxin from *Actinia equina*, J. Biol. Chem. 279 (2004) 34209–34216.
[15] B.B. Bonev, Y.-H. Lam, G. Anderluh, A. Watts, R.S. Norton, F. Separovic, Effects of the eukaryotic pore-forming cytolysin equinatoxin II on lipid membranes and the role of sphingomyelin, Biophys. J. 84 (2003) 2382–2392.
[16] G. Anderluh, A. Razpotnik, Z. Podlesek, P. Maček, F. Separovic, R.S. Norton, Interaction of the eukaryotic pore-forming cytolysin equinatoxinII with model membranes: ^{19}F NMR studies, J. Mol. Biol. 347 (2005) 27–39.
[17] N. Poklar, J. Fritz, P. Maček, G. Vesnaver, T.V. Chalikian, Interaction of the pore-forming protein equinatoxin II with model lipid membranes: a calorimetric and spectroscopic study, Biochemistry 38 (1999) 14999–15008.
[18] G. Menestrina, V. Cabiaux, M. Tejuca, Secondary structure of sea anemone cytolysins in soluble and membrane bound form by infrared spectroscopy, Biochem. Biophys. Res. Commun. 254 (1999) 174–180.
[19] G. Anderluh, A. Barlič, C. Potrich, P. Maček, G. Menestrina, Lysine 77 is a key residue in aggregation of equinatoxin II, a pore-forming toxin from sea anemone *Actinia equina*, J. Membr. Biol. 173 (2000) 47–55.
[20] J.M.M. Caaveiro, I. Echabe, I. Gutiérrez-Aguirre, J.L. Nieva, J.L.R. Arrondo, J.M. González-Mañas, Differential interaction of equinatoxin II with model membranes in response to lipid composition, Biophys. J. 80 (2001) 1343–1353.
[21] J. Alegre-Cebollada, A. Martínez del Pozo, J.G. Gavilanes, E. Goormaghtigh, Infrared spectroscopy study on the conformational changes leading to pore formation of the toxin sticholysin II, Biophys. J. 93 (2007) 3191–3201.
[22] B.A. Wallace, D. Mao, Circular dichroism analyses of membrane proteins: an examination of differential light scattering and absorption flattening effects in large membrane vesicles and membrane sheets, Anal. Biochem. 142 (1984) 317–328.
[23] B.A. Wallace, C.L. Teeters, Differential absorption flattening optical effects are significant in the circular dichroism spectra of large membrane fragments, Biochemistry 26 (1987) 65–70.
[24] A.J. Miles, B.A. Wallace, Synchrotron radiation circular dichroism spectroscopy of proteins and applications in structural and functional genomics, Chem. Soc. Rev. 35 (2006) 39–51.
[25] B.A. Wallace, R.W. Janes, Synchrotron radiation circular dichroism spectroscopy of proteins: secondary structure, fold recognition and structural genomics, Curr. Opin. Chem. Biol. 5 (2001) 567–571.
[26] G. Anderluh, J. Pungerčar, B. Štrukelj, P. Maček, F. Gubenšek, Cloning, sequencing, and expression of equinatoxin II, Biochem. Biophys. Res. Commun. 220 (1996) 437–442.
[27] R.S. Norton, P. Macek, G.E. Reid, R.J Simpson, Relationship between the cytolysins tenebrosin C from *Actinia tenebrosa* and equinatoxin II from *Actinia equina*, Toxicon 30 (1992) 13–23.
[28] J.G. Lees, B.R. Smith, F. Wien, A.J. Miles, B.A. Wallace, CDtool — an integrated software package for circular dichroism spectroscopic data processing, analysis and archiving, Anal. Biochem. 332 (2004) 285–289.
[29] A.J. Miles, F. Wien, J.G. Lees, A. Rodger, R.W. Janes, B.A. Wallace, Calibration and standardisation of synchrotron radiation circular dichroism (SRCD) amplitudes and conventional circular dichroism (CD) spectrophotometers, Spectroscopy 17 (2003) 653–661.
[30] L. Whitmore, B.A. Wallace, DICHROWEB, an online server for protein secondary structure analyses from circular dichroism spectroscopic data, Nucleic Acids Res. 32 (2004) W668–W673.
[31] P. Manavalan, W.C. Johnson Jr, Variable selection method improves the prediction of protein secondary structure from circular dichroism spectra, Anal. Biochem. 167 (1987) 76–85.
[32] I.H.M. Van Stokkum, H.J.W. Spoelder, M. Bloemendal, R. Van Grondelle, F.C.A. Groen, Estimation of protein secondary structure and error analysis from CD spectra, Anal. Biochem. 191 (1990) 110–118.
[33] N. Sreerama, R.W. Woody, Estimation of protein secondary structure from CD spectra: comparison of CONTIN, SELCON and CDSSTR methods with an expanded reference set, Anal. Biochem. 282 (2000) 252–260.
[34] D. Mao, E. Wachter, B.A. Wallace, Folding of the H^+-ATPase proteolipid in phospholipid vesicles, Biochemistry 21 (1982) 4960–4968.
[35] J.G. Lees, A.J. Miles, F. Wien, B.A. Wallace, A reference database for circular dichroism spectroscopy covering fold and secondary structure space, Bioinformatics 22 (2006) 1955–1962.
[36] B.A. Wallace, F. Wien, T.C. Stone, A.J. Miles, J.G. Lees, R.W. Janes, A circular dichroism reference database for membrane proteins, Biophys. J. 90 (2006) 317a.
[37] M. Gandhavadi, D. Allende, A. Vidal, S.A. Simon, T.J. McIntosh, Structure, composition, and peptide binding properties of detergent soluble bilayers and detergent resistant rafts, Biophys. J. 82 (2002) 1469–1482.
[38] C. Wolf, K. Koumanova, B. Tenchov, P.J. Quinn, Cholesterol favors phase separation of sphingomyelin, Biophys. Chem. 89 (2001) 163–172.
[39] O. Bakht, P. Pathak, E. London, Effect of the structure of lipids favoring disordered domain formation on the stability of cholesterol-containing ordered domains (lipid rafts): identification of multiple raft-stabilization mechanisms, Biophys. J. 93 (2007) 4307–4318.
[40] G. Cevc, Appendix B: thermodynamic parameters of phospholipids, in: G. Cevc (Ed.), Phospholipids Handbook, Marcel Dekker, New York, 1993, pp. 939–956.
[41] B.A. Cornell, G.C. Fletcher, J. Middlehurst, F. Separovic, Temperature dependence of the size of phospholipid vesicles, Biochim. Biophys. Acta 642 (1981) 375–380.
[42] B.A. Cornell, G.C. Fletcher, J. Middlehurst, F. Separovic, The lower limit to the size of small sonicated phospholipid vesicles, Biochim. Biophys. Acta 690 (1982) 15–19.
[43] B.A. Wallace, J. Lees, A.J.W. Orry, A. Lobley, R.W. Janes, Analyses of circular dichroism spectra of membrane proteins, Protein Sci. 12 (2003) 875–884.
[44] N.P. Cowieson, A.J. Miles, G. Robin, J.K. Forwood, B. Kobe, J.L. Martin, B.A. Wallace, Evaluating protein:protein complex formation using synchrotron radiation circular dichroism spectroscopy, Prot. Struct. Funct. Bioinformatics 70 (2008) 1142–1146.
[45] A. Drechsler, C. Potrich, J. Sabo, M. Frisanco, G. Guella, M. Dalla Serra, G. Anderluh, F. Separovic, R.S. Norton, Structure and activity of the N-terminal region of the eukaryotic cytolysin equinatoxin II, Biochemistry 45 (2006) 1818–1828.